Lawrence Berkeley National Laboratory

LBL Publications

Title

Heat Vulnerability Index Development and Mapping

Permalink

https://escholarship.org/uc/item/0bz3m9p0

Authors

Xu, Yujie

Hong, Tianzhen

Zhang, Wanni

et al.

Publication Date

2024-01-21

Peer reviewed

eScholarship.org Powered by the California Digital Library
University of California

SimAUD 2021
SYMPOSIUM ON SIMULATION FOR ARCHITECTURE + URBAN DESIGN

Heat Vulnerability Index Development and Mapping

Yujie Xu, Tianzhen Hong, Wanni Zhang, Zhaoyun Zeng, Max Wei

Lawrence Berkeley National Laboratory, Berkeley, USA
{thong, mwei}@lbl.gov

ABSTRACT

Extreme heat is one of the leading causes of weather-related deaths in the U.S. Exposure to extreme heat will be exacerbated due to global climate change. It is thus crucial to design a key performance indicator, heat vulnerability index (HVI), to represent overall heat risk which can help identify susceptible regions and sub-populations in cities in the face of heatwaves. Most existing HVI tools only consider outdoor heat exposure. This paper developed an HVI web map tool incorporating both the outdoor and the indoor heat exposure, as well as population sensitivity and adaptation capability across census tracts in the city of Fresno, California. The tool can assist the planning of infrastructure and resources to reduce residents' vulnerability to extreme heat events. (Available at https://citybes.lbl.gov/?hvi=1).

Author Keywords

Extreme heat; vulnerable population; climate; resilience; geographical information system.

ACM Classification Keywords

•Information systems~Information systems applications~Decision support systems~Data analytics•Human-centered computing~Visualization~Visualization application domains~Geographic visualization•Computing methodologies~Modeling and simulation

1 INTRODUCTION

Extreme heat could cause diseases like hyperthermia, heat exhaustion, and heatstroke [1]. Increased apparent temperature is associated with elevated all-cause mortality [2], especially for certain subgroups defined by age, social-economic status, and pre-existing health conditions [2–5].

Climate change will increase the frequency, duration, and severity of heat waves. By mid-century, the average temperature across the continental U.S. is projected to increase by 1.4ºC, with a higher increase in the annual daily maximum of 2.8ºC, and an even higher increase in heatwave temperature of 6-7ºC [6]. This could pose additional challenges in the mitigation of heat-related health and economic damages.

This study aims to develop an HVI and mapping tool to visualize the vulnerability across census tracts in the city of Fresno, California, by aggregating factors identified in epidemiology literature and other heat vulnerability assessment tools.

2 DATA

2.1 Data Sources

Following [7–9], the vulnerability to extreme heat is characterized in three aspects: environmental exposure, population sensitivity, and adaptation capacity. Exposure quantifies the severity of extreme heat. Sensitivity reflects demographics and pre-existing health condition that increases the risk of developing worse outcomes under similar heat exposure. Adaptation indicates factors that modify the level of heat exposure or sensitivity. A sub-index is developed for each of the three aspects. Table 1 summarizes the data input fields, summary statistics, and their sources.

Sub-Index	Variable	Time	Mean (range)	Source
Environmental Exposure	Number of hours with the heat index in the "danger" or "extreme danger" range	2018 summer	73.83 (13—155)	[10]
	Longest number of consecutive heat-wave days		5.63 (1—10)	
	Number of heat-wave days (daily maximum temperature above 30 ºC, and daily minimum temperature above 22ºC)		11.08 (1-—18)	
	Annual mean PM2.5 concentration	2011	14.13 (12.82—14.99)	[11]
	The three-year ozone average concentration above the state standard	2011	0.34 (0.21—0.46)	

© 2021 Society for Modeling & Simulation International (SCS)

Sub-Index	Variable	Time	Mean (range)	Source
	Building heat resistance indicator, a simulation-based metric reflecting indoor heat exposure of a typical summer day	July 15th from TMY3 weather data	4.55 (3.07—6.52)	Derived in the project
Population Sensitivity	Percent of population over 65	2013—2017	11.68 (0.1—42.4)	[12]
	Percent of population under 5		8.39 (0—17.8)	
	Percent of the population without a high school degree		25.41 (1.9—66.6)	
	Percent of the population below the poverty level threshold		28.44 (1.4—77.3)	
	Percent non-white population		70.77 (29—98.9)	
	Percent of population with ambulatory disability		8.38 (2.4—31.7)	
	Asthma hospitalization rate per 10,000 people		85.4 (20.55—142.28)	
	Heart attack rate per 1,000 people	2013	9.77 (3.14—17.15)	[11]
	Percent of population with a cognitive disability	2013	6.69 (1.3—25.8)	
Adaptation Capacity	Median income	2013—2017	48.4 (12.47—126.25)	[12]
	Percent of the census tract area covered in parks	2020	1.17 (0—22.98)	[13]

Table 1 Data Source and Summary Statistics

2.2 Spatial Distribution of HVI Inputs

Environmental Exposure

Figure 1 shows the spatial distribution of six exposure inputs. The total number of excessive-heat days indicates high heat exposure in the southeast side of the city, while the total number of hours with high heat index indicates center and west, due to the elevated high RH from the green space and the river in the northwest side of the city. In this analysis, excessive-heat days consider only high-temperature exposure, while the heat index metric involves both the temperature and the relative humidity. PM2.5 concentration is higher in the south and is lower in the north, while ozone pollution is more severe in the center. All six measures have some overlapping high exposure in the center of the city.

Population Sensitivity

The elderly population is concentrated in the north end of the city. The population with low education, under poverty, and are non-white are spatially correlated, and are more concentrated in the center and south of the city. Figure 2 visualizes four of the demographic inputs related to the sensitivity to severe damage in extreme heat events.

The population in the central and south of the city also has a higher heart attack rate and asthma ER visits. The hot spots for cognitive disability and ambulatory disabilities are more evenly spread out across the whole city. Figure 3 compares the four pre-existing inputs related to the pre-existing health condition.

Adaptation Capacity

The lower-income population is concentrated in the center and south of the city, while a higher concentration of green space is on the west and north side of the city (Figure 4).

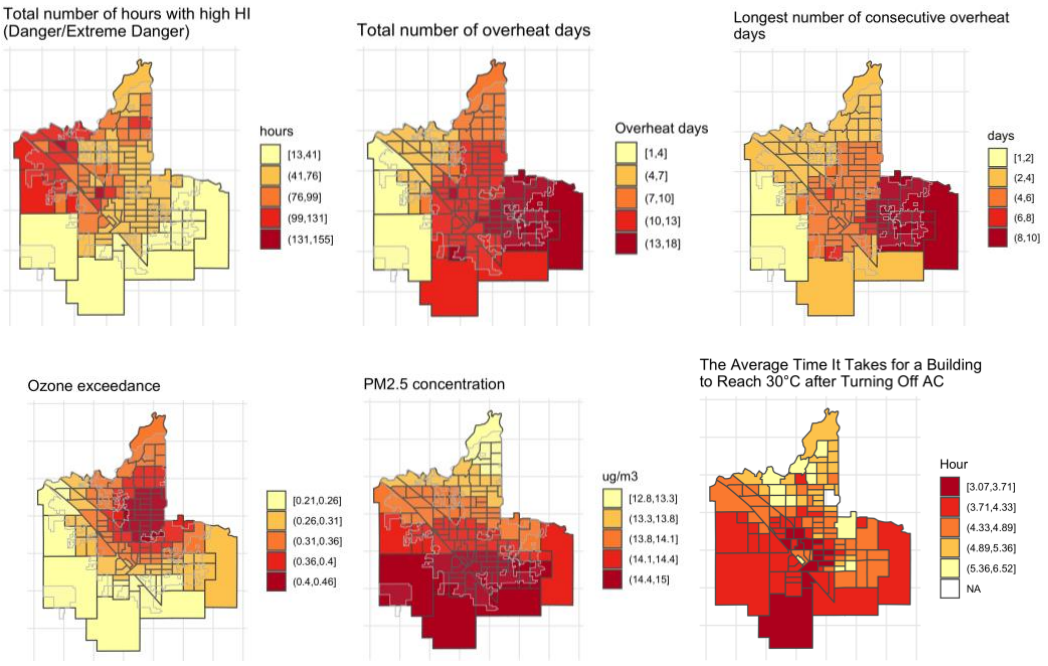

Figure 1 Heat and pollution exposure across census tracts in the city of Fresno

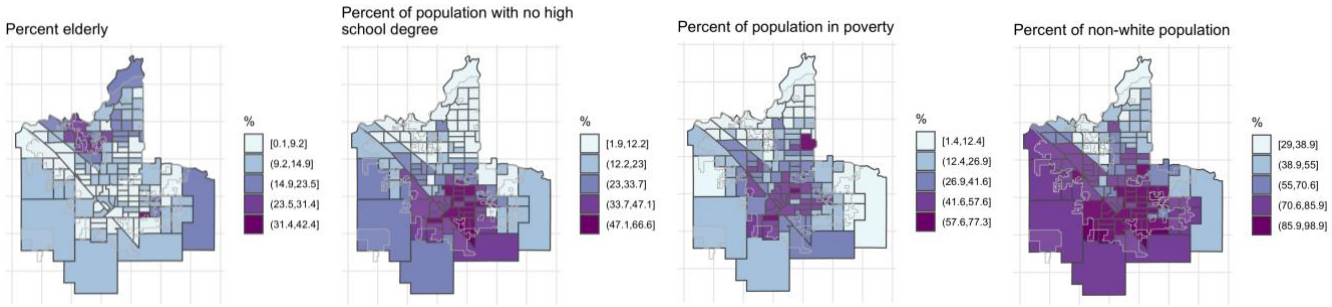

Figure 2 Demographics-related sensitivity factors across census tracts in the city of Fresno

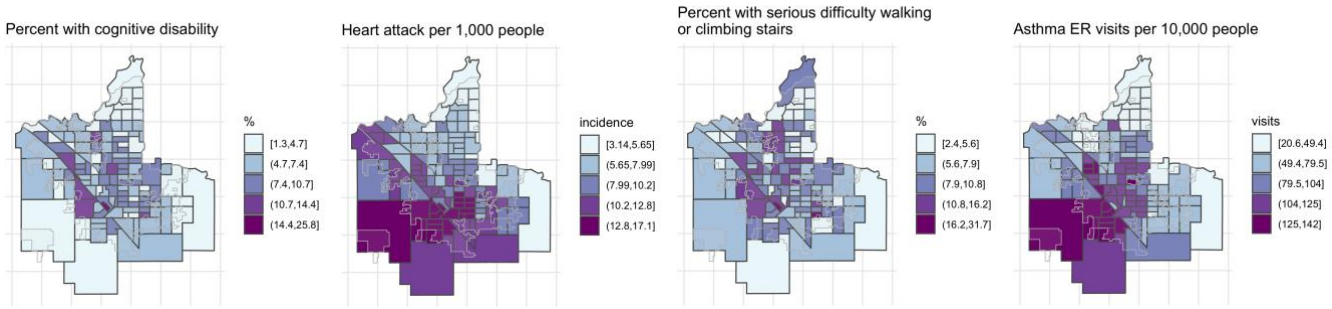

Figure 3 Pre-existing health condition across census tracts in the city of Fresno

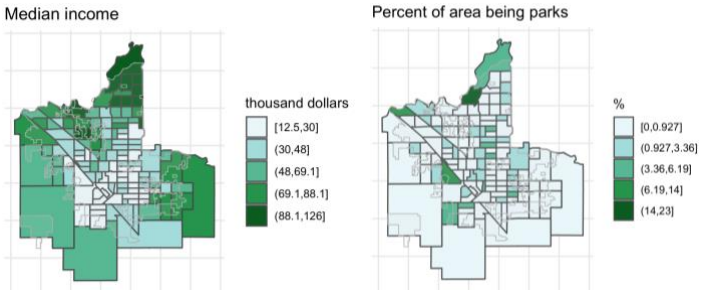

Figure 4 Median income and availability of open green space across census tracts in the city of Fresno

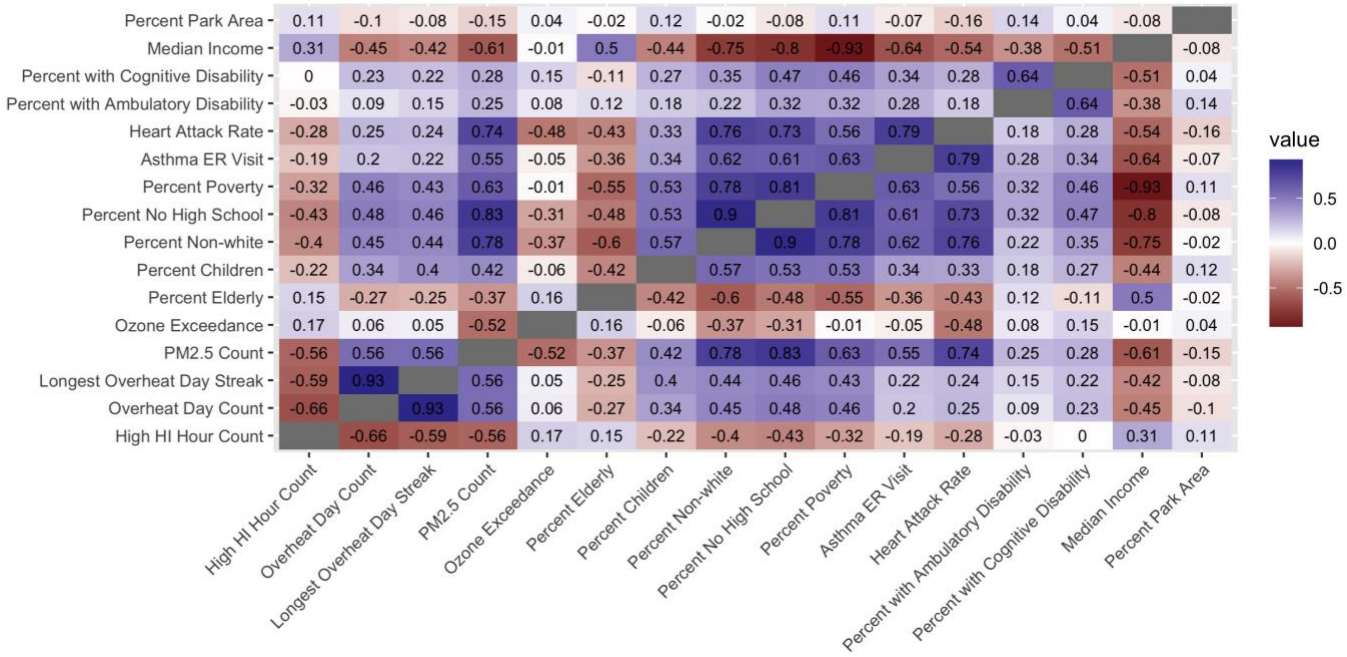

Figure 5 Spearman's rank correlation coefficient

Correlation between HVI inputs

With a pair-wise correlation analysis, it is observed that excessive-heat days and longest excessive-heat day streak are more correlated with PM2.5 concentration (Spearman's $\rho = 0.56$) than ozone exceedance (Spearman's $\rho < 0.1$). Percent of the non-white population is highly correlated with low education (Spearman's $\rho = 0.9$), and poverty (Spearman's $\rho = 0.81$). These three factors are also correlated with high PM2.5, with a correlation coefficient of 0.63-0.83. Asthma ER visits rate and heart attack rate are also positively correlated with the percent of low education, non-white, and poverty, with a correlation coefficient of 0.61-0.76. Across all variables, percent of the population with no high school degree, percent non-white population, and PM2.5 concentration have the highest average correlation with other input features. Figure 5 shows the Spearman's rank correlation coefficient estimates for each pair of HVI inputs.

3 HVI CONSTRUCTION

3.1 The Three Sub-indices

The Exposure sub-index consists of three outdoor and one indoor heat exposure factor, and two air pollution factors. Hourly weather data (temperature, relative humidity, wind speed, etc.) during the summer months of 2018 is retrieved for 26 weather stations from Weather Underground [10]. The weather measurements of a census tract are computed with an inverse distance weighted average of corresponding measurements of nearby weather stations, within 6.2 miles (10km) of the census tract centroid. Due to the interaction between heat and air and pollution [14, 15], PM2.5 and ozone concentration are included as two other exposure factors. The building heat resistance indicator predicts the indoor heat exposure level from a series of building characteristics. This metric will be described in more detail in Section 3.2.

The Sensitivity sub-index addresses the increased heat-related morbidity and mortality due to age, socioeconomic status, and pre-existing health conditions. According to

epidemiology literature, elderly above 65 [3] or 75 [2], children below 5 [3], black [3] or non-whites [5], and people under poverty or with low education [4] are associated with greater risk of mortality due to elevated temperature. Other studies found no significant association between education and heat-related mortality [3]. Pre-existing health condition is another risk indicator for heat-related death. Excessive heat is associated with higher mortality in cardiovascular diseases [3], increased asthma ER visits among children [16], and asthma hospitalization among adults [17].

The Adaptation sub-index consists of two factors, income and the availability of outdoor green space. These factors could increase survivability during an extreme heat event. For example, low income is associated with an increased mortality rate during hot weather [2]. Green space could mitigate the urban heat island effect and is included in several existing HVI tools and studies [7, 18].

3.2 Building Heat Resistance Indicator

A building heat resistance indicator is developed to represent how well a building responds to outdoor heat when there is no air conditioning that causes the indoor temperature to rise. A building with high heat resistance is able to curb the indoor temperature to rise slowly due to its capability to reduce heat transfer from the outside, which depends on the thermal performance of the building envelope (walls, roofs, windows, airtightness, exterior shading) as well as the building orientation and thermal mass. This factor is generated through building simulation. Since there are around 120,000 residential buildings in Fresno, due to limited resources, 4361 buildings from four neighborhoods of Fresno city are selected to be simulated. The date selected for simulation is July 15th from TMY3 weather data, a typical summer weekend with a maximum temperature of 38.1ºC. All buildings start with an indoor air temperature controlled at the setpoint of 25.6 ºC. Then the power for HVAC is switched off at 9 a.m. The time (in hours) that each building takes to reach an indoor air temperature of 30 ºC is used as the indicator of its heat resistance. Figure 6 shows the temperature change of all simulated buildings.

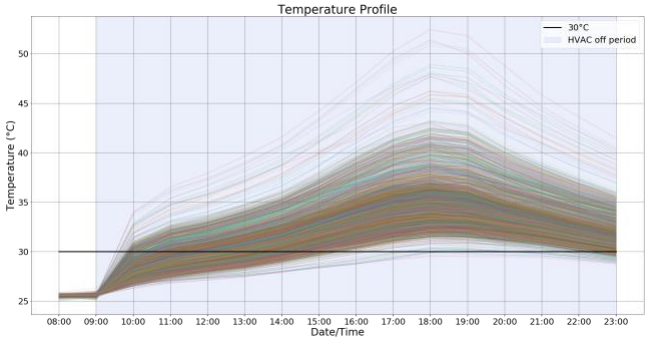

Figure 6 The temperature profile of all simulated buildings for heat resistance indicator

To generalize the results to all buildings in Fresno, a linear regression model is fitted to build the relationship between the time constant and several input variables, including the building type, the number of stories, the vintage, the footprint area, the ratio of the window facing east and west, the number of shading buildings and the number of touching buildings. The time constant of all buildings in Fresno is then predicted by the regression model, and the heat resistance indicator is generated based on the distribution of the time constant. The bottom right plot in Figure 1 visualizes the average time constant for buildings in each census tract.

3.3 Web Interface

The Web tool in this study visualizes three separate HVI sub-indices (exposure, sensitivity, and adaptation), and an aggregated overall HVI. Figure is a screenshot of the interface showing the exposure sub-index. The four views can be toggled with buttons on the top right (component 1). In the exposure view, the individual input factors are shown as small maps on the right (component 4). The value of each input factor is discretized into five classes using the Jenks natural breaks, and are labeled as 1 to 5, indicating the severity of the corresponding variable. The 1-5 class labels are then aggregated into the exposure index (Component 2) with a weighted average. Users can specify the weights in the text box below the corresponding input (Component 4).

The HVI mapping tool is a feature of the urban environment of CityBES [19], an open data and computing platform for city buildings, energy, and sustainability (available at CityBES.lbl.gov).

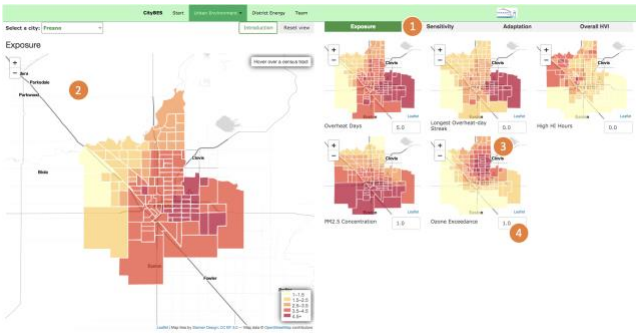

Figure 7 The web interface of the HVI tool

4 RESULTS

This section presents the spatial distribution of the three sub-indices, and the overall HVI when individual factors are aggregated with equal weights.

4.1 Environmental Exposure

The environmental exposure is higher in the center and southeast of the city and is lower in the north and northwest. Figure 8. This is a result of a large number of excessive-heat days, and a high concentration of PM2.5 and ozone.

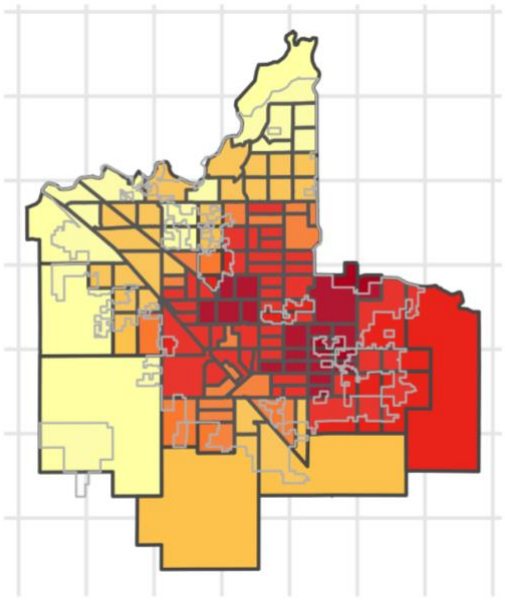

Figure 8 Environmental exposure map

4.2 Spatial Distribution of Population Sensitivity

The sensitivity sub-index is also highest in the center and south of the city (Figure 9). This is due to both the high percentage of socially disadvantaged groups (low education, high poverty level, and non-white), and pre-existing conditions of cardiovascular diseases and asthma. The worse pre-existing conditions might also be linked to worse air quality.

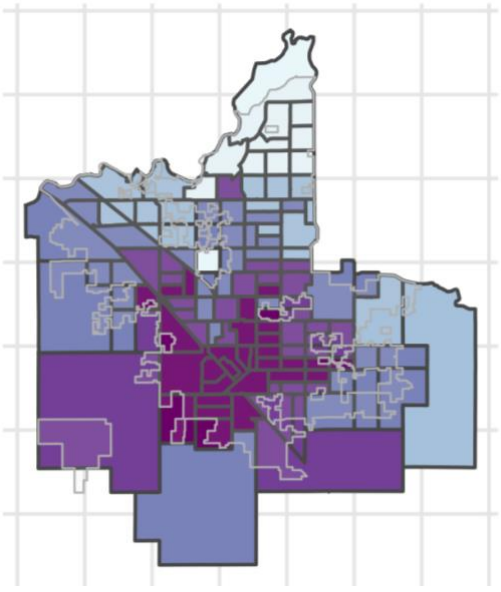

Figure 9 Population sensitivity map

4.3 Spatial Distribution of Adaptation Capacity

Contrary to the exposure and sensitivity, the adaptation capacity is lowest in the center of the city and higher in the north and near the city boundary (Figure 10).

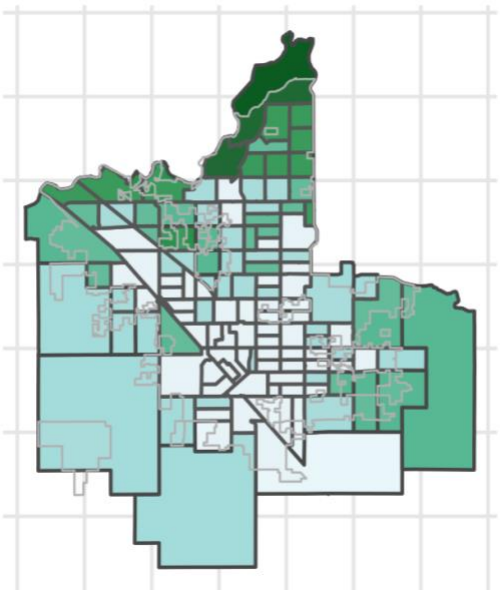

Figure 10 Adaptation capacity map

4.4 Overall HVI

Overall, the aggregated HVI shows the highest vulnerability in the center and south part of the city (Figure 11), due to high environmental exposure, dense socially disadvantaged population, poor pre-existing health conditions, and low adaptation capacity from both economic status and green space availability.

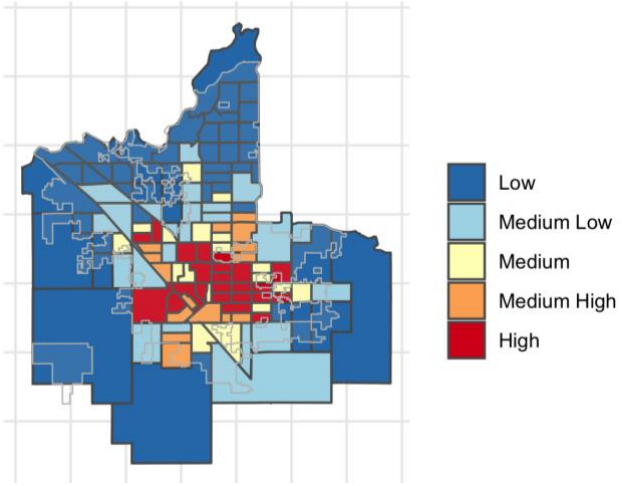

Figure 11 Overall HVI map

5 DISCUSSION

This study aims to develop a map tool visualizing the overall and three aspects of the vulnerability to extreme heat events across census tracts in the city of Fresno, California.

In our analysis of HVI across census tracts in the city of Fresno, sizable correlations are found between poverty, low education, and poor pre-existing health conditions. Similar correlations are also found in previous studies between poverty and low education [20, 21], poverty and percent of non-white population, percent elderly living alone, and

prevalence of diabetes in [21]. The central part of the city is found to be the most vulnerable area in the city, with high environmental exposure, high social vulnerability, and low adaptation capacity. Such high vulnerability in the center of the city is also found in previous studies, for example [20, 22]. This highlights the importance of addressing the urban heat island effect and social inequality, in the mitigation of damages from elevated temperatures.

Many existing studies aim to present an aggregated single heat vulnerability index [8, 20–22]. However, according to [9], to assist the response planning to extreme heat events, the heat vulnerability indicator should vary with the corresponding intervention, rather than giving only a global measure. For example, when designing the heat warning system, the vulnerability indicator should focus more on environmental exposure. On the other hand, in the planning of public facilities or green space that could act as a shelter to heatwaves, the social vulnerability and the availability of public transportation should be weighted more heavily. Other emerging public health concerns might also influence the feasibility of various adaptation strategies. For example, to lower the risk of COVID-19 transmission, indoor cooling centers such as libraries, community centers, or shopping malls are either with restricted access or temporarily closed. This might make it more desirable to increase outdoor cooling centers, such as public parks, or to add passive cooling features to individual homes, such as cool roofs. In the allocation of healthcare resources in extreme heat events, pre-existing health conditions and age groups should be weighted more heavily.

The current tool has a few limitations. First, due to data availability, some important factors are not accounted for in the current heat vulnerability map. Such factors include AC availability, homeless population, car ownership, and many other important pre-existing health condition indicators including diabetes, respiratory diseases, etc. Moreover, how closely the index provided by the tool match the actual heat-related health or economic damage is not verified due to limited data availability of heat-related hospitalization and mortality.

6 CONCLUSION

Heatwaves or high-temperature exposure can result in increased morbidity and mortality [2], and other worsened economic outcomes [23]. With climate change and increased frequency and intensity of future heatwaves, response to extreme heat will become increasingly important for local and national resilience planning. This motivates the development of a mapping tool to visualize the local heat vulnerability. The tool provides both an aggregated single vulnerability indicator, and three sub-indicators highlighting three different aspects of heat vulnerability: environmental exposure, population sensitivity, and adaptation capacity. To facilitate the design of different heat mitigation strategies, the tool allows users to customize the weights of individual factors. The study found a high vulnerability in the center of the city, with more severe heat and pollution exposure, a high percentage of the socially disadvantaged population, and poor pre-existing health conditions. This suggests that addressing the urban heat island effect and social inequality are important in the design of resilience to extreme heat events.

ACKNOWLEDGMENTS

We thank the project team members and stakeholders for reviewing the tool and providing valuable feedback. We gratefully acknowledge the grant from California Strategic Growth Council.

REFERENCES

1. CDC, “Heat-related illness,” Apr. 2017.
2. M. Stafoggia *et al.*, “Vulnerability to Heat-Related Mortality: A Multicity, Population-Based, Case-Crossover Analysis,” *Epidemiology*, vol. 17, no. 3, pp. 315–323, 2006, https://doi.org/10.1097/01.ede.0000208477.36665.34
3. R. Basu and B. D. Ostro, “A Multicounty Analysis Identifying the Populations Vulnerable to Mortality Associated with High Ambient Temperature in California,” *Am. J. Epidemiol.*, vol. 168, no. 6, pp. 632–637, Sep. 2008, https://doi.org/10.1093/aje/kwn170
4. F. C. Curriero, K. S. Heiner, J. M. Samet, S. L. Zeger, L. Strug, and J. A. Patz, “Temperature and Mortality in 11 Cities of the Eastern United States,” *Am. J. Epidemiol.*, vol. 155, no. 1, pp. 80–87, Jan. 2002, https://doi.org/10.1093/aje/155.1.80.
5. J. Schwartz, “Who is sensitive to extremes of temperature? A case-only analysis,” *Epidemiology*, pp. 67–72, 2005, https://doi.org/10.1097/01.ede.0000147114.25957.71.
6. D. J. Wuebbles, D. W. Fahey, and K. A. Hibbard, “Climate science special report: fourth national climate assessment, volume I,” 2017, [Online]. Available: https://science2017.globalchange.gov/chapter/6/.
7. San Francisco Climate and Health Program, “San Francisco Vulnerability to the Health Impacts of Extreme Heat,” 2019. https://sfgov.maps.arcgis.com/apps/MapJournal/index.html?appid=093e26ddb26a4e3180fa1e35158858bf (accessed Aug. 17, 2020).
8. Q. Zhu *et al.*, “The spatial distribution of health vulnerability to heat waves in Guangdong Province, China,” *Glob. Health Action*, vol. 7, no. 1, p. 25051, 2014, https://doi.org/10.3402/gha.v7.25051.
9. C. Rinner, D. Patychuk, K. Bassil, S. Nasr, S. Gower, and M. Campbell, “The role of maps in neighborhood-level heat vulnerability assessment for the city of Toronto,” *Cartogr. Geogr. Inf. Sci.*, vol. 37, no. 1, pp. 31–44, 2010, https://doi.org/10.1559/152304010790588089.

10. TWC Product and Technology LLC, “Weather History & Data Archive,” *Weather Underground*, Aug. 2020. https://www.wunderground.com/history (accessed Aug. 17, 2020).
11. Four Twenty Seven, “The California Heat Assessment Tool: Planning for the Health Impacts of Extreme Heat,” Aug. 2018. [Online]. Available: http://427mt.com/wp-content/uploads/2018/08/427-CHAT-report.pdf.
12. U.S. Census Bureau, “2013-2017 American Community Survey 5-Year Estimates,” 2017. https://www.census.gov/newsroom/press-kits/2017/acs-5-year.html.
13. City of Fresno, “City of Fresno Data Hub,” 2020. https://gis-cityoffresno.hub.arcgis.com/ (accessed Aug. 17, 2020).
14. C. Ren, G. M. Williams, L. Morawska, K. Mengersen, and S. Tong, “Ozone modifies associations between temperature and cardiovascular mortality: analysis of the NMMAPS data,” *Occup. Environ. Med.*, vol. 65, no. 4, pp. 255–260, Apr. 2008, https://doi.org/10.1136/oem.2007.033878.
15. M. S. O’Neill, A. Zanobetti, and J. Schwartz, “Modifiers of the Temperature and Mortality Association in Seven US Cities,” *Am. J. Epidemiol.*, vol. 157, no. 12, pp. 1074–1082, Jun. 2003, https://doi.org/10.1093/aje/kwg096.
16. Z. Xu, C. Huang, W. Hu, L. R. Turner, H. Su, and S. Tong, “Extreme temperatures and emergency department admissions for childhood asthma in Brisbane, Australia,” *Occup. Environ. Med.*, vol. 70, no. 10, pp. 730–735, Oct. 2013, https://doi.org/10.1136/oemed-2013-101538.
17. S. Soneja, C. Jiang, J. Fisher, C. R. Upperman, C. Mitchell, and A. Sapkota, “Exposure to extreme heat and precipitation events associated with increased risk of hospitalization for asthma in Maryland, U.S.A.,” *Environ. Health*, vol. 15, no. 1, p. 57, Apr. 2016, https://doi.org/10.1186/s12940-016-0142-z.
18. New York State Department of Health, “Heat Vulnerability Index,” *New York State Department of Health*, Jul. 2020. https://www.health.ny.gov/environmental/weather/vulnerability_index/index.htm (accessed Aug. 17, 2020).
19. T. Hong, Y. Chen, S. H. Lee, and M. A. Piette, “CityBES: A web-based platform to support city-scale building energy efficiency,” *Urban Comput.*, vol. 14, 2016.
20. C. Reid *et al.*, “Mapping Community Determinants of Heat Vulnerability,” *Environ. Health Perspect.*, vol. 117, no. 11, pp. 1730–1736, Nov. 2009, https://doi.org/10.1289/ehp.0900683.
21. G. Maier, A. Grundstein, W. Jang, C. Li, L. P. Naeher, and M. Shepherd, “Assessing the Performance of a Vulnerability Index during Oppressive Heat across Georgia, United States,” *Weather Clim. Soc.*, vol. 6, no. 2, pp. 253–263, Apr. 2014, https://doi.org/10.1175/WCAS-D-13-00037.1.
22. T. Wolf and G. McGregor, “The development of a heat wave vulnerability index for London, United Kingdom,” *Weather Clim. Extrem.*, vol. 1, pp. 59–68, Sep. 2013, https://doi.org/10.1016/j.wace.2013.07.004.
23. M. Dell, B. F. Jones, and B. A. Olken, “What do we learn from the weather? The new climate-economy literature,” *J. Econ. Lit.*, vol. 52, no. 3, pp. 740–98, 2014, https://doi.org/ 10.1257/jel.52.3.740.